

## Supplementary Material for

# Synthesis and characterization of $^{89}\text{Zr}$ -labeled AGuIX nanoparticles

Charles Truillet<sup>1,†</sup>, Eloise Thomas<sup>2,†</sup>, Francois Lux<sup>2</sup>, Loc. T. Huynh<sup>1</sup>, Olivier Tillement<sup>2</sup>, Michael J. Evans<sup>1,\*</sup>

<sup>1</sup>Department of Radiology and Biomedical Imaging, University of California San Francisco, 185 Berry Street, Lobby 6, Suite 350, San Francisco CA 94107, <sup>2</sup>Institut Lumiere Latière, UMR5306, Université Claude Bernard Lyon1-CNRS, Université de Lyon 69622 Villeurbanne cedex, France.

<sup>†</sup>These authors contributed equally

\*To whom the correspondence should be addressed:

Michael J. Evans, PhD. email: Michael.evans@ucsf.edu, 415-353-3442

## Supplemental Methods :

**Chemicals:** Sodium hydroxide (NaOH, 99.99%), hydrochloric acid (HCl, 36.5–38%) and dimethylsulfoxide (DMSO, >99.5%) were purchased from Aldrich Chemical (France), acetonitrile (CH<sub>3</sub>CN, >99.9%) was purchased from Carlo Erba (France), trifluoroacetic acid (TFA, >99%) was purchased from Alfa Aesar (United Kingdom), copper sulfate pentahydrate (CuSO<sub>4</sub>·5H<sub>2</sub>O, 98%) was purchased from Merck (Germany). AGuIX particles were purchased from Nano-H (Saint-Quentin Fallavier, France). The desferrioxamine chelate, p-NCS-Bz-DFO (N1-hydroxy-N1-(5-(4-(hydroxy(5-(3-(4-isothiocyanatophenyl)thioureido)pentyl)amino)-4-oxobutanamido)pentyl)-N4-(5-(N-hydroxyacetamido)pentyl)succinamide) was purchased from ChemaTech (Dijon, France). All products were used without further purification. Only Milli-Q water ( $\rho > 18 \text{ M}\Omega \cdot \text{cm}$ ) was used for the aqueous solution preparation.

**Elemental Analysis:** The determination of Gd, C, N and Si contents of particles was performed by the Filab compagny (France) by ICPMS (precision : 0.5%). For DFO-AGuIX, the massic percentage is 10.7 for Gd, 10.4 for Si, 26.15 for C and 7.78 for N. This is consistent with the following average composition for DFO-AGuIX :  $(\text{Gd}_1\text{APTES}^*_{2.78}\text{TEOS}^*_{2.66}\text{DOTAGA}^*_{1.02}\text{DFO}^*_{0.14}) \cdot x \text{H}_2\text{O}$ . APTES\*, TEOS\*, DOTAGA\* and DFO\* refer to the corresponding molecules that have reacted and actually present within the nanoparticle.

**Relaxivity measurements:** Relaxation time measurements were performed using a Bruker Minispec MQ60 NMR analyser, operating at 1.4 T magnetic field and 37°C. Before measurements of T1 (longitudinal relaxation time) and T2 (transverse relaxation time), lyophilized particles were dispersed in water for one hour at room temperature,  $[\text{Gd}^{3+}] = 100 \text{ mM}$  and pH=7.4. For AGuIX,  $r_1 = 12.2 \text{ s}^{-1} \cdot \text{mM}^{-1}$  per  $\text{Gd}^{3+}$  and  $r_2 = 16.3 \text{ s}^{-1} \cdot \text{mM}^{-1}$  per Gd. For DFO-AGuIX,  $r_1 = 16.7 \text{ s}^{-1} \cdot \text{mM}^{-1}$  per  $\text{Gd}^{3+}$  and  $r_2 = 24.6 \text{ s}^{-1} \cdot \text{mM}^{-1}$  per  $\text{Gd}^{3+}$ .

**Dynamic Light Scattering size measurement:** Direct measurements of the hydrodynamic diameter distribution of the nanoparticles were performed *via* a Zetasizer NanoS DLS (laser He-Ne 633 nm) from Malvern Instruments. For measurements, lyophilized particles were first dispersed in water for one hour at room temperature,  $[\text{Gd}^{3+}] = 100 \text{ mM}$  and pH=7.4. Then particles were diluted to  $[\text{Gd}^{3+}] = 10 \text{ mM}$  and measurements immediately taken. The average hydrodynamic diameter (in number) measured by DLS was  $3.6 \pm 0.8 \text{ nm}$  for AGuIX and  $4.4 \pm 1 \text{ nm}$  for DFO-AGuIX.

**High performance liquid chromatography:** Gradient HPLC analysis was done by using a Shimadzu® Prominence series UFLC system with a CBM-20A controller bus module, an LC-20AD liquid chromatograph, a CTO-20A column oven, an SPD-20A UV-visible detector and an RF-20A fluorescence detector. UV-visible absorption was measured at 295 nm for particles characterization or 700 nm for free chelates quantification (UV-visible absorption single wavelength detection). 20  $\mu\text{L}$  of the sample were loaded in the solvent injection ratio: 99% solvent A–1% solvent C (A = Milli-Q water–TFA 99.9 : 0.1 v/v; C = CH<sub>3</sub>CN–TFA 99 : 9.1 : 0.1 v/v/v) onto a Jupiter C4 column (150 × 4.60 mm, 5  $\mu\text{m}$ , 300 Å, Phenomenex®) at a flow rate of 1  $\text{mL} \cdot \text{min}^{-1}$  for 7 min. In a second step, samples were eluted by a gradient developed from 1 to

90% of solvent C for 15 min. The concentration of solvent C was maintained for 7 min. Then, the concentration of solvent C was decreased to 1% for a period of 1 min followed by an additional 8 min at this final concentration to re-equilibrate the system. Before each sample measurement, a baseline was performed following the same conditions by loading Milli-Q water into the injection loop. For measurements, lyophilized particles were first dispersed in water for one hour at room temperature,  $[Gd^{3+}] = 100$  mM and  $pH = 7.4$ . Then particles were diluted to  $[Gd^{3+}] = 5$  mM and immediately injected for measurement. AGuIX have a retention time of 12.98 min, a width at half height of 0.99 min and a purity of 91 %. DFO-AGuIX has a retention time of 15.21 min, a width at half height of 0.83 min and a purity of 99 %.

Free chelates quantification: DFO-AGuIX particles were dispersed in water at a concentration of  $[Gd^{3+}] = 100$  mM for 1h at room temperature. Then different samples were prepared by adding to particles an increasing quantity of a  $Cu^{2+}$  solution in order to have a concentration of  $Gd^{3+}$  equal to 38.4 mM in each sample and a concentration of  $Cu^{2+}$  from 0 to 19 mM. Samples were let stand for 24 h at room temperature and finally injected without any dilution for HPLC analysis (UV-visible absorption was measured at 700 nm). The area of peaks at 2.4 min (unbound  $Cu^{2+}$ ), at 3-5 min (small degradation by-products that have chelated  $Cu^{2+}$ ) and at 15.2 min ( $Cu^{2+}$  complexed to DFO-AGuIX) were determined.

Biological half-life determination: The biological half-life of  $^{89}Zr$ -DFO-AGuIX was determined in tumor naïve *nu/nu* mice. Mice ( $n = 4$ ) were injected with  $\sim 200$  mCi of the radiotracer, and total internal radioactivity was determined as a function of time over 3 half-lives of zirconium-89. The data were normalized to the total internal activity at the time of injection, and curve fitting with PRISM was used to determine the  $t_{1/2(eff)}$ . The  $t_{1/2(bio)}$  was determined with the following equation:

$$t_{1/2, eff} = \frac{t_{1/2} t_{1/2, bio}}{t_{1/2} + t_{1/2, bio}}$$

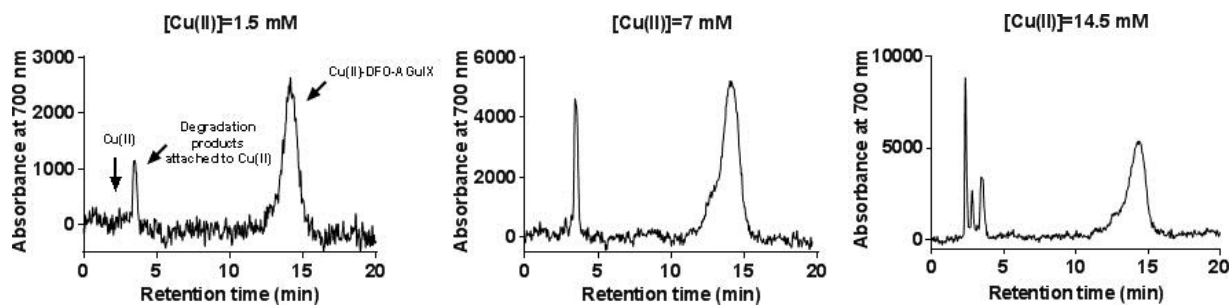
Propagation of cell lines: The human glioblastoma cell line U87MG was purchased from ATCC and cultured according to manufacturer's recommendations.

Biodistribution studies: At a dedicated time after radiotracer injection, animals were euthanized by  $CO_2(g)$  asphyxiation, and 14 tissues (including the tumor) were removed, rinsed in water, dried in air for 5 min, weighed and counted on a gamma-counter for accumulation of  $^{89}Zr$ -radioactivity. The mass of radiotracer formulation injected into each animal was measured and used to determine the total number of counts (counts per minute, [c.p.m.]) by comparison to a standard syringe of known activity and mass. Count data will be background- and decay-corrected and the tissue uptake measured in units of percentage injected dose per gram (%ID/g) will be calculated by normalization to the total amount of activity injected.

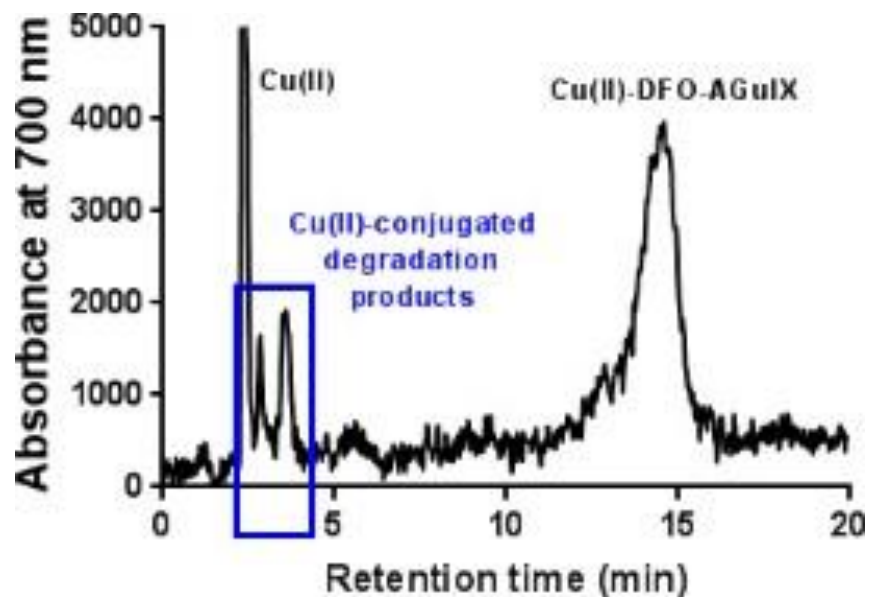
Autoradiography: Following euthanasia, tumor tissues were excised and covered by OCT mounting medium (Sakura Finetek, Torrance, CA), frozen on dry ice, and a series of 8  $\mu m$  thick frozen sections cut with a Leica facility. To determine radiotracer distribution, digital autoradiography was performed by placing tissue sections in a film cassette against a phosphor imaging plate (Molecular Dynamics) for 24 h at  $-20$  °C. Phosphor imaging plates were read at a

pixel resolution of 88  $\mu\text{m}$  with a phosphorimager 445 SI (Molecular Dynamics). After autoradiographic, exposure, the same frozen sections were then used for histology staining and imaging.

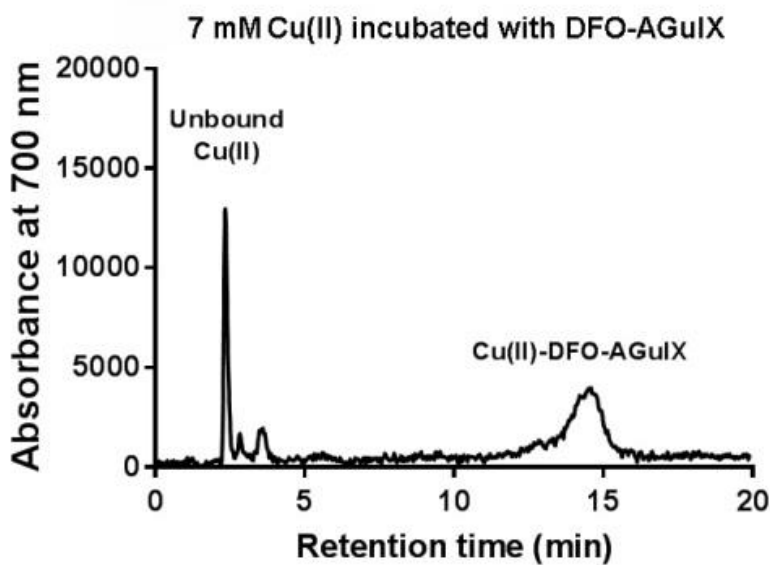
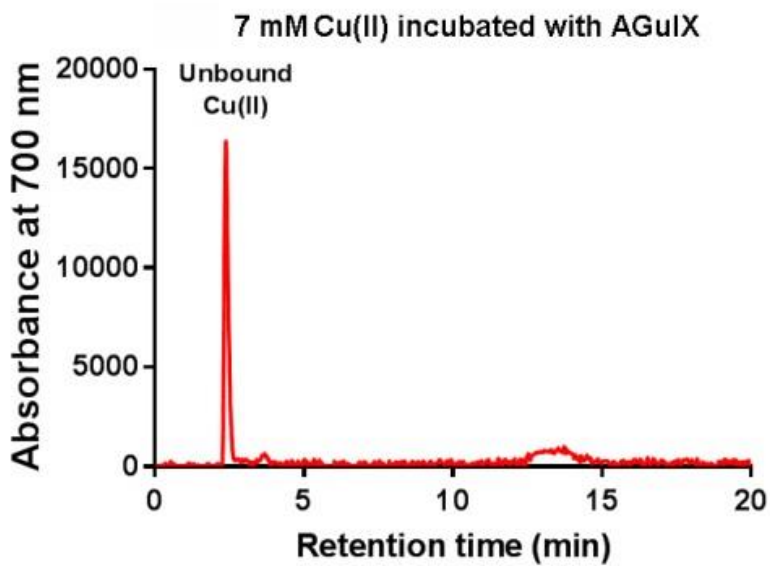
Supplemental Figure 1 : Representative HPLC traces showing the  $\text{Cu}^{2+}$  associated species after incubation with DFO-AGuIX and sub- or saturating doses of Cu(II) sulfate. The nanoparticle was incubated at 38.4 mM with respect to [Gd].



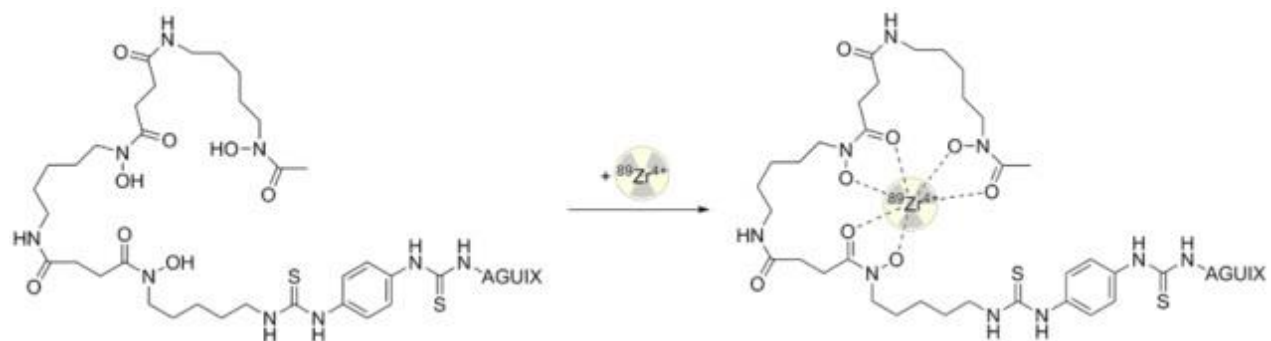
Supplemental Figure 2. A representative HPLC trace showing a magnified view of the Cu(II)-associated degradation products consistently observed in incubations with DFO-AGuIX in vitro. The degradation products are highlighted in a blue box.



Supplemental Figure 3. Representative HPLC data showing the results of an incubation of 7 mM Cu(II) sulfate with AGuIX (DFO-free) and DFO-AGuIX. Both nanoparticles were incubated at 38.4 mM with respect to [Gd].

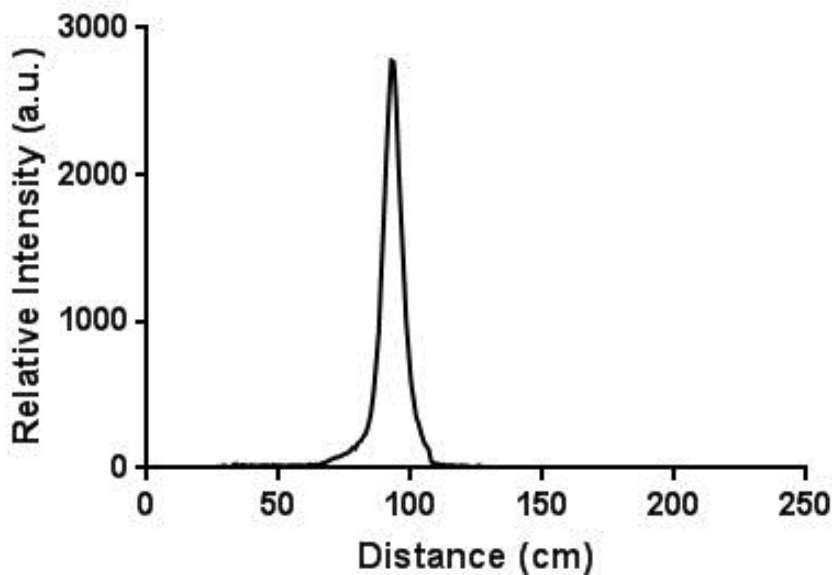


Supplemental Figure 4. A schema showing the radiolabeling of DFO-AGuIX with  $^{89}\text{Zr}^{4+}$ .

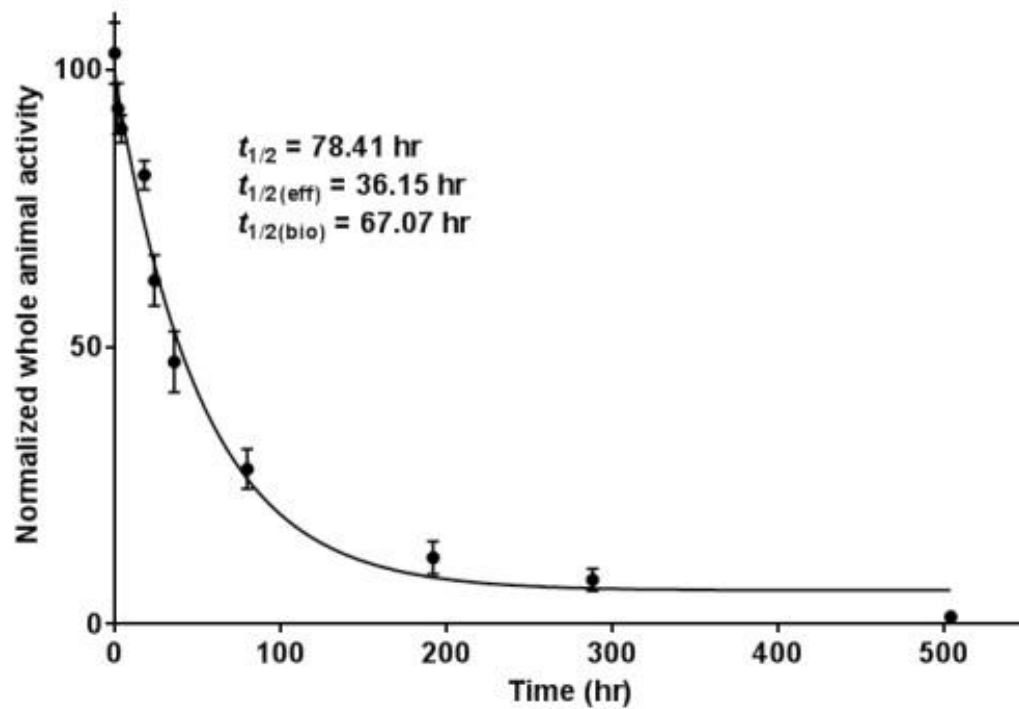


Supplemental Figure 5: A representative iTLC showing the migration of free  $^{89}\text{Zr}$ -oxalate with a mobile phase of 20 mM citric acid and 20 mM sodium carbonate. The peak clearly resolved from  $^{89}\text{Zr}$ -DFO-AGuIX.

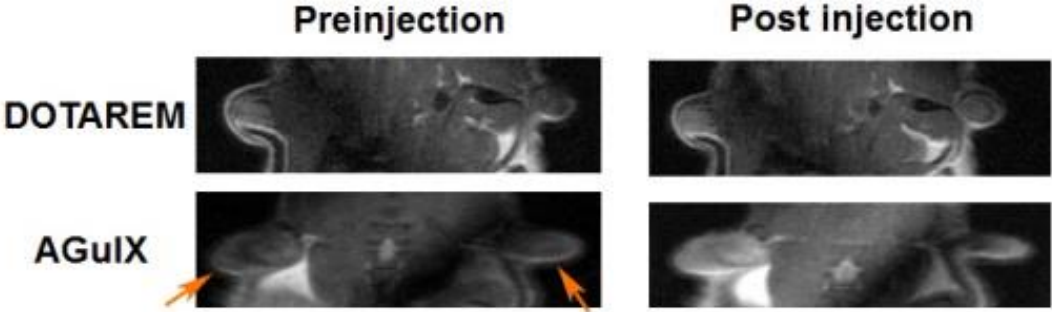
### iTLC of $^{89}\text{Zr}$ -oxalate with citric acid mobile phase



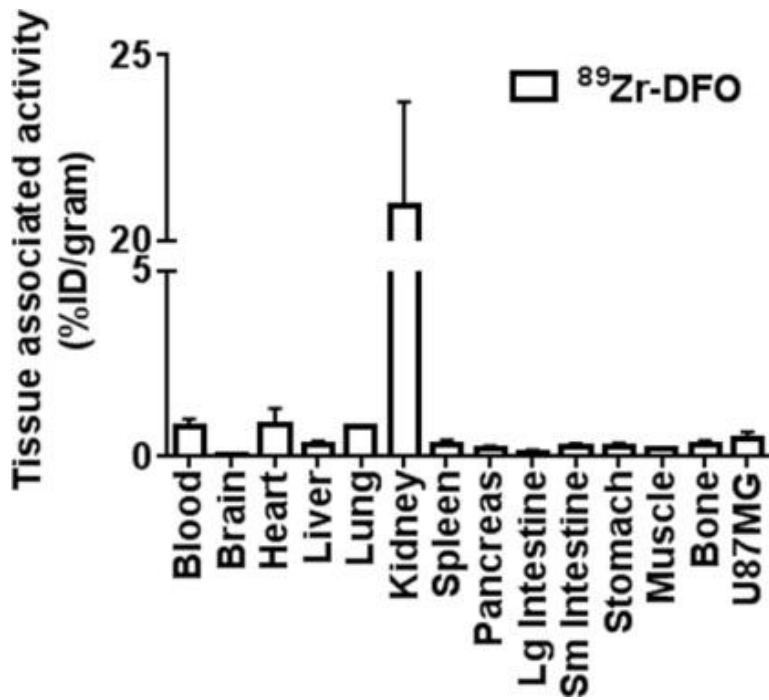
Supplemental Figure 6: A representation of the data used to determine the biological half-life of  $^{89}\text{Zr}$ -DFO-AGuIX in normal mice. The data was fit to a one phase exponential decay curve, and the biological half-life was calculated from the effective half-life.  $R^2 = 0.95$



Supplemental Figure 6: Representative MRI images from mice treated with  $^{89}\text{Zr}$ -DFO-AGuIX and DOTAREM® showing contrast due to intratumoral accumulation of  $^{89}\text{Zr}$ -DFO-AGuIX. The orange arrows indicate the location of the U87MG tumors.

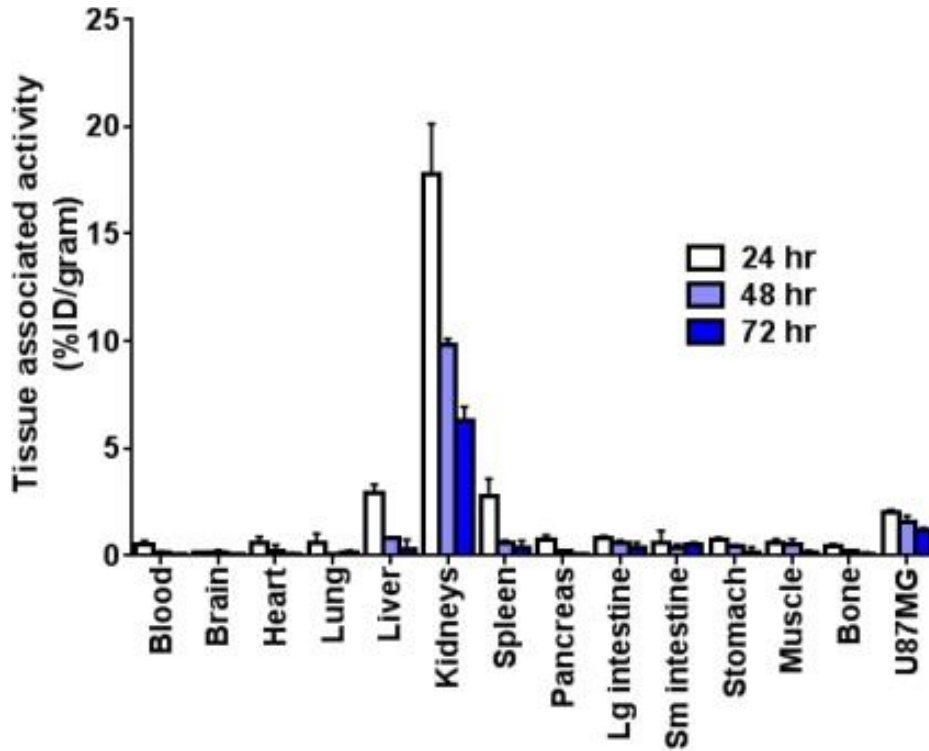


Supplemental Figure 7: Biodistribution data from a larger panel of normal tissues and tumor in mice treated with  $^{89}\text{Zr}$ -DFO. The data was acquired 24 hours post injection.



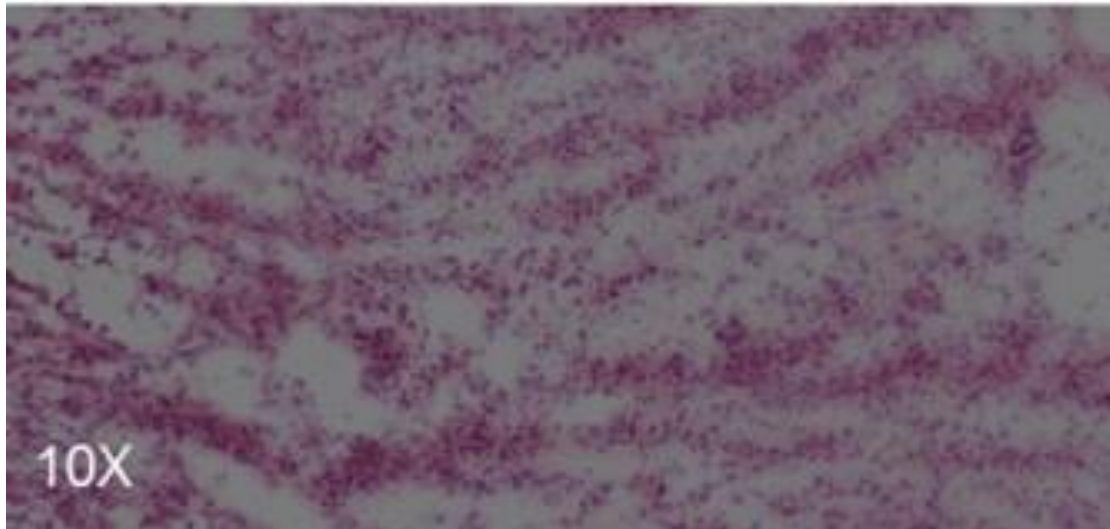
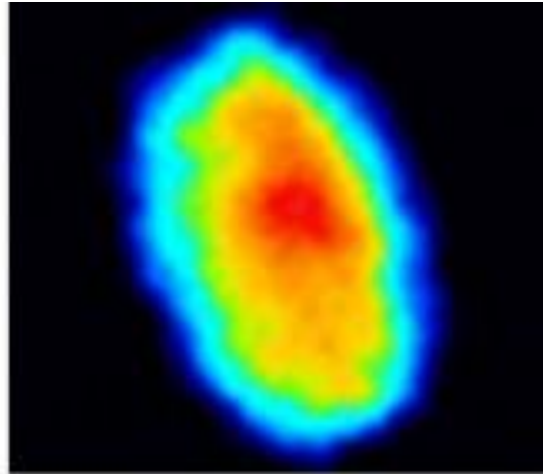
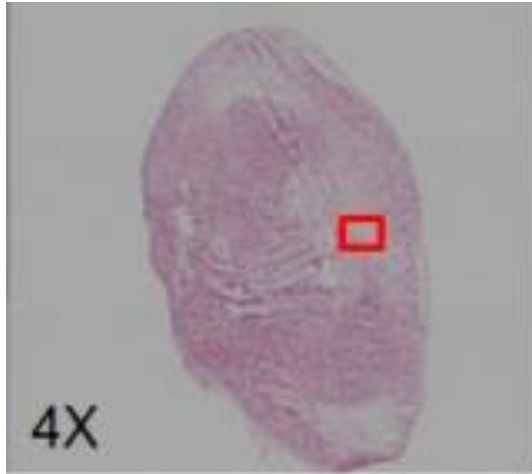
Tissue	24 hours		
Blood	0.9	1.0	0.6
Brain	0.1	0.0	0.1
Heart	1.1	1.2	0.3
Liver	0.4	0.4	0.3
Lung	0.8	0.8	0.8
Kidney	24.1	18.8	19.9
Spleen	0.4	0.4	0.2
Pancreas	0.3	0.2	0.1
Lg Intestine	0.1	0.2	0.1
Sm Intestine	0.4	0.3	0.2
Stomach	0.3	0.3	0.1
Muscle	0.2	0.3	0.2
Bone	0.4	0.2	0.4
U87MG	0.7	0.4	0.4

Supplemental Figure 8: Biodistribution data from a larger panel of normal tissues and tumor in mice treated with <sup>89</sup>Zr-DFO-AGuIX. The data was acquired 24, 48, and 72 hours post injection.

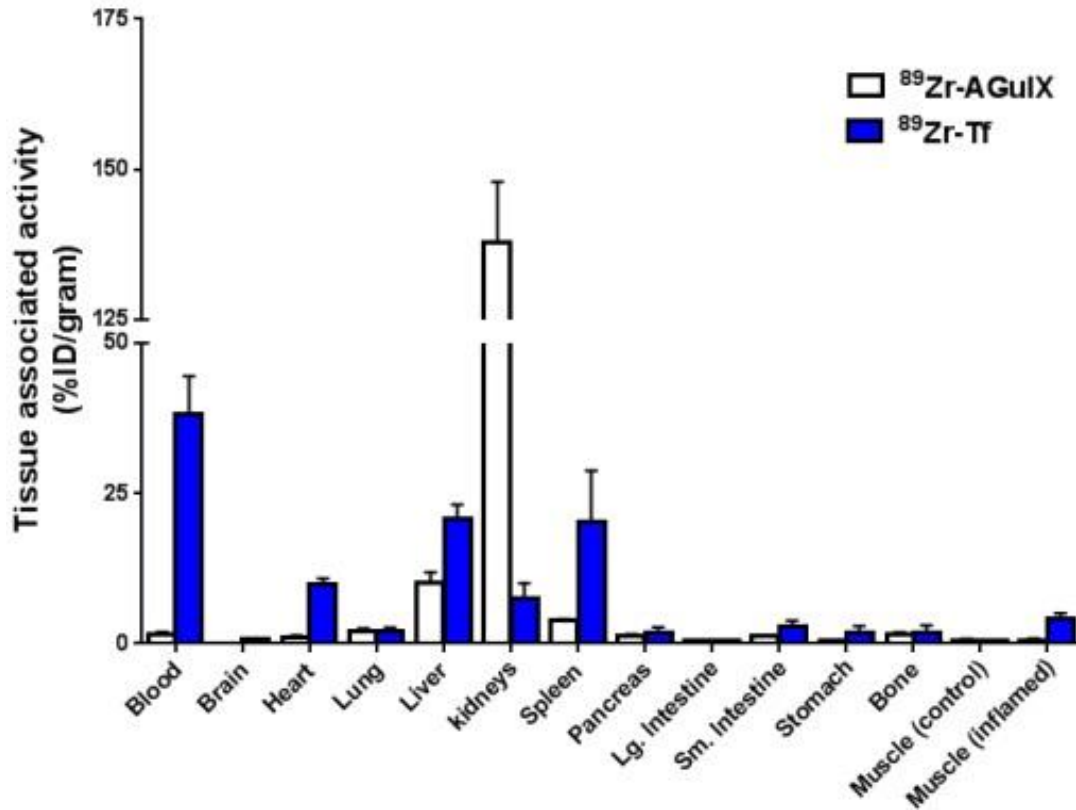


Tissue	24 hours			48 hours			72 hours		
Blood	0.7	0.6	0.4	0.2	0.1	0.2	0.1	0.1	0.1
Brain	0.1	0.2	0.1	0.1	0.3	0.0	0.0	0.1	0.0
Heart	0.3	0.7	0.8	0.1	0.5	0.1	0.1	0.1	0.1
Lung	1.0	0.7	0.2	0.1	0.1	0.0	0.0	0.1	0.3
Liver	2.9	3.3	2.6	0.8	0.8	0.8	0.8	0.1	0.0
Kidneys	15.5	17.5	20.2	9.6	10.1	9.7	6.0	5.8	7.0
Spleen	3.7	2.5	2.1	0.7	0.5	0.6	0.8	0.2	0.2
Pancreas	0.7	1.0	0.5	0.2	0.2	0.2	0.1	0.0	0.0
Lg intestine	0.9	0.9	0.7	0.7	0.5	0.5	0.5	0.5	0.1
Sm intestine	0.0	1.1	0.8	0.5	0.5	0.2	0.6	0.6	0.4
Stomach	0.9	0.7	0.6	0.4	0.4	0.5	0.4	0.0	0.0
Muscle	0.5	0.4	0.8	0.2	0.7	0.6	0.0	0.3	0.1
Bone	0.5	0.3	0.5	0.2	0.2	0.2	0.0	0.1	0.1
U87MG	2.2	2.0	1.9	1.9	1.4	1.5	1.2	1.3	1.1

Supplemental Figure 9: Autoradiography of tissue slices from U87MG tumors shows  $^{89}\text{Zr}$ -DFO-AGuIX activity embedded within the pericellular space of the tumor.  $^{89}\text{Zr}$ -DFO-AGuIX circulated for 72 hours in the mouse before these sections were acquired. The image of the H&E stained tissue is represented at 4X and 10X for clarity, while the autoradiography is presented at 4X. The red box indicates the region of interest represented at 10X.



Supplemental Figure 10: Biodistribution data from a larger panel of normal tissues and the inflamed muscle in mice treated with turpentine and  $^{89}\text{Zr}$ -DFO-AGuIX or  $^{89}\text{Zr}$ -DFO-transferrin. The data were acquired 30 min post injection.



Tissue	[ $^{89}\text{Zr}$ ]-AGuIX			[ $^{89}\text{Zr}$ ]-transferrin		
	1	2	3	1	2	3
Blood	2.0	1.1	1.2	31.1	43.1	40.4
Brain	0.1	0.1	0.1	0.7	0.9	0.8
Heart	1.3	0.6	1.2	8.8	10.2	10.7
Lung	1.8	2.1	2.5		1.7	2.5
Liver	8.8	12.1	9.6	18.8	23.3	20.5
Kidney	126.0	144.4	142.9	8.3	4.9	9.7
Spleen	3.9	4.0	4.1	16.9	14.0	30.0
Pancreas	1.1	1.2	1.6	2.1	0.7	2.6
Lg. Intestine	0.4	0.5	0.5	0.5	0.5	0.5
Sm. Intestine	1.1	1.2	1.2	3.6	3.1	1.5
Stomach	0.6	0.5	0.5	1.1	1.3	3.1
Bone	1.5	1.3	1.9	0.2	2.7	2.3
Muscle (control)	0.7	0.4	0.7	0.6	0.6	0.6
Muscle (inflamed)	0.9	0.5	0.4	3.6	4.1	5.1